Boundary Effects in the One-Dimensional Coulomb Gas

D. S. Dean,[1] R. R. Horgan,[2] and D. Sentenac[3]

We use the functional integral technique of Edwards and Lenard to solve the statistical mechanics of a one-dimensional Coulomb gas with boundary interactions leading to surface charging. The theory examined is a one-dimensional model for a soap film. Finite-size effects and the phenomenon of charge regulation are studied. We also discuss the disjoining pressure for such a film. Even in the absence of boundary potentials we find that the presence of a surface affects the physics in finite systems. In general we find that in the presence of a boundary potential the long-distance disjoining pressure is positive, but may become negative at closer interplane separations. This is in accordance with the attractive forces seen at close separations in colloidal and soap film experiments and with three dimensional calculations beyond mean field. Finally, our exact results are compared with the predictions of the corresponding Poisson–Boltzmann theory which is often used in the context of colloidal and thin liquid film systems.

1. INTRODUCTION

Up until 1961 the statistical mechanics of the classical one-dimensional Coulomb gas was an unsolved problem. At more or less the same time the problem was solved by Lenard[2] and independently by Prager.[3] A powerful alternative method of solution using functional integration was subsequently expounded by Lenard and Edwards.[1] A good review of this work

---

[1] CNRS-Laboratoire de Physique Théorique de l'ENS, 75231 Paris Cedex 05, France.

[2] Department of Applied Mathematics and Theoretical Physics, University of Cambridge, Cambridge, CB3 9EW, U.K.

[3] Service de Physique de l'Etat Condensé, CEA, Saclay, 91911, Gif-sur-Yvette Cedex, France.

may be found in ref. 4. It should be mentioned here that the two dimensional Coulomb gas may also be solved exactly at the temperature where $e^2/kT = 2$; this exactly soluble case has been investigated in the electric double layer geometry by Cornu and Jancovici.[7] The problem of electrostatic interactions is one of profound importance in the theory of colloidal stability and also in the understanding of thin liquid films. In these problems one considers the behavior of an electrolytic fluid between two surfaces which either model the surface of large colloidal particles or the surfaces of the thin liquid film. The charging mechanism of the surfaces is usually of a statistical mechanical origin. For example in soap films made from sodium dodecyl sulphate (SDS), the soap anions have hydrocarbon tails which are hydrophobic and hence have a preference to lie on the surface of the film.[12] In colloidal systems chemical reactions may occur between the colloid particles and the surrounding electrolytic medium again leading to surface charging. As the two planes are brought together surface charge regulation occurs. The precise qualitative behavior is still only understood within the context of mean field Poisson–Boltzmann type theories,[8, 9] and at a more sophisticated level using the hyper-netted chain approximation (HNC). Rather surprisingly the HNC theory predicts, in the context of colloidal systems, that the electrostatic interactions between the planes may become attractive for small separations;[5, 6] this is supported by calculations of the fluctuations about the mean field solutions.[14] In the mean field model applied to soap films charge regulation is predicted,[12] but no attractive component is seen to appear within the electrostatic interactions. Interestingly the point at which charge regulation becomes important in the mean field model for SDS soap films coincides with the range at which collapse to a Newton Black Film (NBF) occurs.[12] There is much indirect evidence that the transition from a common film to a NBF is of first order, for example it is believed to be exothermic and occurs via a nucleation process where regions of black film expand over the surface of the film. In this paper we propose to analyze the exactly soluble one-dimensional version of the model proposed in ref. 12. We shall use the method of ref. 1 to solve the problem but we shall highlight the finite-size effects appearing in the problem to gain an understanding of how charge regulation occurs in the model. We shall compare our exact results with those of mean field theory to ascertain, at least in one dimension, the accuracy of the traditional Poisson–Boltzmann mean field approach.

The paper is arranged as follows. We formulate a form of the soap film model used in ref. 12 in one dimension. The problem is solved using the functional integral formalism of ref. 1 and the limit of bulk systems is rederived for the sake of completeness. We then analyze the problem in the case of finite films with surface binding interactions and discuss the nature of

the charge regulation and the stability criterion for the one-dimensional film. We then compare the mean field Poisson–Boltzmann theory with the exact results. Finally we conclude with a brief comparison between the qualitative behavior observed in the one-dimensional system and that of experiments.

2. THE MODEL AND ITS PATH INTEGRAL SOLUTION

Here we shall summarize the approach of ref. 1 and apply it to the system in which we are interested. The physical picture to bear in mind is that of a line of charged particles in $[0, L]$ (the film) which is connected to an infinite bulk reservoir. In the model of ref. 1, the bulk is to the left of the system and interacts with the system electrostatically; in addition the entire system, bulk plus film, is taken to be electroneutral. In our model one may imagine that the two one-dimensional systems are embedded in a higher dimensional (say 2D) space and there is a free flow between the two systems, however the electrostatic interaction between the bulk and the film is taken to be such that the film and bulk are individually electroneutral. This condition of electroneutrality for the film is one that is assumed in many contexts and is important for determining the boundary conditions for the nonlinear Poisson–Boltzmann equations in mean field approaches.[8, 9] If one considers a system of charged particles i with coordinates x_i on the real line and of charge $z_i e$, the electrostatic energy of a given configuration is given by the Hamiltonian

$$\mathscr{H}_E = -\frac{e^2}{4} \sum_{i,j} |x_i - x_j| \, z_i z_j \tag{2.1}$$

with $\sum_i z_i = 0$, the electroneutrality condition we impose. The condition of electroneutrality can be justified by considering that the bulk and the film are embedded in a two dimensional space and interact via a one-dimensional electrostatic potential along the y-axis at a distance y, this adds an additional term $(e^2/4) \, y (\sum_i z_i)^2$ to $\mathscr{H}_E$ and in the limit of large y imposes electroneutrality. Using the relation

$$|x - x'| = x + x' - 2 \min(x, x') \tag{2.2}$$

and the condition of electroneutrality we obtain

$$\mathscr{H}_E = \frac{e^2}{2} \sum_{i,j} \min(x_i, x_j) \, z_i z_j \tag{2.3}$$

Hence the electrostatic component of the Boltzmann weight of a particular configuration with the electroneutrality constraint may be written as

$$P[\mathbf{x}] = \frac{e\beta^{1/2}}{2\pi} \int_0^{2\pi/e\beta^{1/2}} d\psi_0 \exp\left[-\frac{\beta e^2}{2} \sum_{i,j} \min(x_i, x_j) z_i z_j + i\beta^{1/2} e\psi_0 \sum_i z_i \right]$$

$$(2.4)$$

where we have used the Fourier representation of the electroneutrality constraint, i.e.

$$\delta_{0,\sum z_i} = \frac{e\beta^{1/2}}{2\pi} \int_0^{2\pi/e\beta^{1/2}} \exp\left(ie\beta^{1/2}\psi_0 \sum z_i \right) d\psi_0 \qquad (2.5)$$

Consider now a standard Brownian motion $\psi(x)$ with time indexed on $[0, L]$ such that $\psi(0) = \psi_0$. We have therefore that

$$E(\psi(x)) = \psi_0 \qquad (2.6)$$

and

$$E(\psi(x)\,\psi(y)) = \psi_0^2 + \min(x, y) \qquad (2.7)$$

where E indicates the expectation over the standard Wiener measure. This means that Eq. (2.4) may be written as an expectation over the paths of the process $\psi(x)$ as

$$P[\mathbf{x}] = \frac{e\beta^{1/2}}{2\pi} \int_0^{2\pi/e\beta^{1/2}} d\psi_0\, E\left(\exp\left[ie\beta^{1/2} \sum_i \psi(x_i) z_i \right] \right) \qquad (2.8)$$

The field theory to model a soap line is now derived from a model consisting of a monovalent soap molecules whose anions are attracted to the surface of the soap film by the presence of an effective potential $V(x)$ which acts on them and whose support is localized at the two adjacent surfaces of the film. In addition one may add an additional monovalent electrolytic species. In the grand canonical ensemble if the fugacities for the soap anions/cations and the electrolyte anions/cations are given by μ_s and μ_e respectively, then the partition function is given by ref. 1

$$Z = \frac{1}{N} \int d[\psi] \exp\left[-\frac{1}{2} \int \left(\frac{d\psi}{dx}\right)^2 dx \right.$$

$$+ \mu_s \int \left(\exp(-i\beta^{1/2} e\psi - \beta V(x)) + \exp(i\beta^{1/2} e\psi) \right) dx$$

$$\left. + 2\mu_e \int \cos(\beta^{1/2} e\psi)\, dx \right] \qquad (2.9)$$

where N is a normalization factor to be determined and the integrals in the path integral are implicitly between 0 and L. The above may be derived by using the link with the Brownian motion ψ above and then rewriting the problem in path integral notation (i.e., by making explicit the Wiener measure). A more general (in the sense that it applies in any dimension) derivation of the representation above, comes from the introduction of the field ψ as a Hubbard Stratonovich field. In general dimension the field theory is a form of the Sine–Gordon field theory and is not generally soluble. For simplicity we shall choose the form of $V(x)$ to be such that

$$\exp(-\beta V(x)) = 1 + \lambda^* \delta(x) + \lambda^* \delta(x - L) \qquad (2.10)$$

i.e., the effective surface potential is highly localized about the boundary points 0 and L. The λ^* appearing in (2.10) is similar to the adhesivity introduced by Davies[10] in his analysis of the surface tensions of hydrocarbon solution, although the idea of such a surface active term goes back to Boltzmann. For physically realizable soap films $V(x)$ is not strictly localized as the effective potential created due to the hydrophobic nature of the soap anion hydrocarbon tails has a support over a region of the length the tail between the surface and the interior of the film (see ref. 12 for a discussion of the mechanism generating this potential). However for the purposes of demonstrating the essential physics of charge regulation in a one-dimensional system our choice of $V(x)$ should be adequate. With this choice of V we obtain

$$Z = \frac{1}{N} \int d[\psi] \exp\left[-\frac{1}{2} \int \left(\frac{d\psi}{dx}\right)^2 dx + 2\mu \int \cos(\beta^{1/2} e\psi) \, dx \right.$$

$$\left. + \lambda(\exp(-i\beta^{1/2} e\psi(0)) + \exp(-i\beta^{1/2} e\psi(L))) \right] \qquad (2.11)$$

with $\mu = \mu_s + \mu_e$ and $\lambda = \mu_s \lambda^*$. Because now the potential V acts only on the end points we may write Z in path integral notation as,

$$Z = \frac{1}{N} \int d\psi_0 \, d\psi_L \int_{\psi(0) = \psi_0}^{\psi(L) = \psi_L} d[\psi] \exp\left[-\frac{1}{2} \int \left(\frac{d\psi}{dx}\right)^2 dx \right.$$

$$\left. + 2\mu \int \cos(\beta^{1/2} e\psi) \, dx + \lambda(\exp(-i\beta^{1/2} e\psi(0)) + \exp(-i\beta^{1/2} e\psi(L))) \right] \qquad (2.12)$$

The path integral is that for a diffusing particle in a cosine potential, consequently following ref. 1 we find

$$Z = \frac{1}{N} \int d\psi_0 \, d\psi_L \, P(\psi_0, \psi_L \mid L) \exp[\lambda(\exp(-i\beta^{1/2}e\psi_0) + \exp(-i\beta^{1/2}e\psi_L))] \tag{2.13}$$

where $P(\psi_0, \psi \mid x)$ obeys

$$\frac{1}{2} \frac{\partial^2 P}{\partial \psi^2} + 2\mu \cos(\beta^{1/2}e\psi) \, P = \frac{\partial P}{\partial x} \tag{2.14}$$

subject to the initial condition $P(\psi_0, \psi \mid 0) = \delta(\psi_0 - \psi)$. Note here that, for the reasons given earlier, the boundary terms ψ_0 and ψ_L in our path integral are free and are integrated over, this is in contrast to the study of ref. 1, where $\psi_0 = 0$ and only ψ_L is left free. Note that the previous discussion of the Brownian process $\psi(x)$ is rather important for precisely determining the boundary conditions in the path integral. In order to determine the normalization factor N we note that when $e = \lambda = 0$ then we should obtain the ideal gas result $Z = \exp(2\mu L)$. In this case

$$P(\psi_0, \psi \mid x) = \frac{1}{(2\pi x)^{1/2}} \exp\left(-\frac{1}{2x}(\psi - \psi_0)^2\right) \exp(2\mu x) \tag{2.15}$$

giving simply

$$Z\big|_{e=\lambda=0} = \frac{1}{N} \int d\psi_0 \exp(2\mu L) \tag{2.16}$$

At this point we must regularize the partition function by bounding the possible values of ψ_0 between two extrema yielding

$$N = \max(\psi_0) - \min(\psi_0) \tag{2.17}$$

In the case where $e \neq 0$ we may use the fact that the action is invariant under translations of $2\pi/e\beta^{1/2}$ to obtain (we have simply assumed that the extremal values of ψ_0 are integer multiples of $2\pi/e\beta^{\frac{1}{2}}$)

$$Z = \frac{e\beta^{1/2}}{2\pi} \int_0^{2\pi/e\beta^{1/2}} d\psi_0 \int_{-\infty}^{\infty} d\psi_L$$

$$\times \exp[\lambda(\exp(-i\beta^{1/2}e\psi_0) + \exp(-i\beta^{1/2}e\psi_L))] \, P(\psi_0, \psi_L \mid L) \tag{2.18}$$

Note that this discussion would have been redundant if we had kept in mind the Brownian formalism above, this would have given us the integration limits on ψ_0 and the value of N directly (and more rigorously!).

A further simplification is obtained by noting that

$$\int P(\psi_0, \psi_L \mid L) \, f(\psi_L) \, d\psi_L = K(\psi_0 \mid L) \qquad (2.19)$$

where $K(\psi_0 \mid L)$ obeys

$$HK = \frac{\partial K}{\partial L} \qquad (2.20)$$

with

$$H = \frac{1}{2} \frac{\partial^2}{\partial \psi_0^2} + 2\mu \, \cos(\beta^{1/2} e \psi_0) \qquad (2.21)$$

subject to the initial condition $K(\psi_0 \mid 0) = f(\psi_0)$. In our problem

$$f(\psi_0) = \exp(\lambda \, \exp(-i\beta^{1/2} e \psi_0)) \qquad (2.22)$$

For simplicity in notation we shall take $\beta = 1$ from here on. To recover the temperature dependence the rescalings as $e^2 \to \beta e^2$ and $P \to kTP$ should be performed. The final expression for Z is

$$Z = \frac{e}{2\pi} \int_0^{2\pi/e} d\psi_0 \, K(\psi_0 \mid L) \, f(\psi_0) \qquad (2.23)$$

which in operator notation may be expressed as

$$Z = \frac{e}{2\pi} \int_0^{2\pi/e} d\psi_0 \, f(\psi_0) \exp(LH) \, f(\psi_0) \qquad (2.24)$$

The pressure of the film is simply given by $P(L) = \partial \log(Z)/\partial L$. The bulk pressure is given by $P_{bulk} = \lim_{L \to \infty} P(L)$ and the disjoining pressure of the film is given by the difference between the film and bulk pressures, i.e.

$$P_d = \frac{\partial}{\partial L} \log(Z) - P_{bulk} \qquad (2.25)$$

Finally defining the field $\phi = e\psi$ we obtain

$$Z = \frac{1}{2\pi} \int_0^{2\pi} d\phi_0 \, f(\phi_0) \exp(LH) \, f(\phi_0) \tag{2.26}$$

where now $f(\phi_0) = \exp(\lambda \exp(-i\phi_0))$ and

$$H = \tfrac{1}{2}e^2 H^* \tag{2.27}$$

where

$$H^* = \frac{\partial^2}{\partial\phi_0^2} + a\cos(\phi_0) \tag{2.28}$$

with $a = 4\mu/e^2$. Physical quantities may be related to observables of the field theory in the standard way by including source terms in the partition function and then taking functional derivatives of $\log(Z)$ with respect to these source terms. One-point observables are calculated as

$$\langle O(\phi(x)) \rangle = \frac{1}{2\pi Z} \int_0^{2\pi} d\phi_0 \, f(\phi_0) \exp(xH) \, O(\phi_0) \exp((L-x)H) \, f(\phi_0) \tag{2.29}$$

the extension to n-point functions being trivial.

3. RESULTS FOR LARGE FILMS: THERMODYNAMIC LIMIT

The eigenfunctions of H^* periodic on $[0, 2\pi]$ are the periodic Mathieu functions $\chi_n(\phi, a)$ whose eigenvalues we denote by $\gamma_n(a)$ and where it is easy to see that the largest eigenvalue $\gamma_0(a) < a$. Hence in the case where $e^2 L/2 \gg 1$

$$Z \sim \frac{1}{2\pi} \left(\int_0^{2\pi} d\phi \, \chi_0(\phi) \, f(\phi) \right)^2 \exp\left(\frac{e^2}{2} L\gamma_0(a) \right) \tag{3.1}$$

therefore $P_{bulk} = (e^2/2)\,\gamma_0(a)$ and any boundary terms become insignificant in the thermodynamic limit.

3.1. Small a, Large e—Strong Coupling Limit

In the case where a is small one may evaluate $\gamma_0(a)$ in perturbation theory and we find that[17]

$$\gamma_0(a) = \frac{1}{2} a^2 - \frac{7}{32} a^4 + \frac{29}{144} a^6 - \frac{68687}{294912} a^8 + \cdots \tag{3.2}$$

In this regime the average density is extensive and is given by

$$p = \mu \frac{\partial P}{\partial \mu} = \frac{e^2}{2} a \frac{dy_0(a)}{da} \tag{3.3}$$

The condition that a is small is therefore equivalent to

$$a \sim \sqrt{2p}/e \ll 1 \tag{3.4}$$

This implies that the electrostatic energy is much greater than the contribution from the entropy. From Eqs. (2.25), (3.2), and (3.3) the pressure is then given by the series

$$P_{bulk} = \frac{1}{2} p \left[1 + \frac{7}{8} \left(\frac{p}{e^2} \right) - \frac{23}{288} \left(\frac{p}{e^2} \right)^2 - \frac{4897}{122288} \left(\frac{p}{e^2} \right)^3 + \cdots \right] \tag{3.5}$$

This result was explained by Lenard as an effect of dimerization. The leading term is independent of e and is the perfect gas result for a density of $p/2$. This is explained by the positive and negative charges binding in pairs to give, in leading order, a neutral gas with half the original particle density. The non-leading terms correspond to multipole interactions such as van der Waals forces etc.

3.2. Large *a*, Small *e*—Weak Coupling Limit

The calculation of $y_0(a)$ for large a can be formulated as a perturbation series for H^* in Eq. (2.28) obtained by expanding the cosine and writing

$$H^* = a + H_{osc} + O(a\phi^4) \tag{3.6}$$

where H_{osc} is the harmonic oscillator Hamiltonian

$$H_{osc} = \frac{\partial^2}{\partial \phi^2} - \frac{1}{2} a\phi^2 \tag{3.7}$$

Thus the perturbation theory is for the anharmonic terms in Eq. (3.6) using the basis of oscillator states associated with H_{osc}. The first term in the pressure is due to the $O(a)$ term in Eq. (3.6) and gives the free gas contribution. The next correction arises from the ground state eigenvalue of the oscillator and is $O(\sqrt{a})$. This is the well-known Debye–Hückel term. We expect a power series in $a^{-1/2}$, but to carry out the perturbative expansion becomes increasingly difficult as the order increases. Instead, we can

formulate the problem as an expansion in Feynman diagrams. A similar approach to the calculation of the electrostatic free energy of a system of fixed charge macroions has been used by Coalson and Duncan[18] and Ben-Tai and Coalson.[19] In the bulk limit we write the Feynman kernel for $\frac{1}{2}H^*$ as

$$Z = \mathcal{K}(L, a) = \frac{1}{N} \int d[\psi] \exp\left(\int_{-L/2}^{L/2} dx \left[-\frac{1}{2}\left(\frac{d\psi}{dx}\right)^2 + \frac{a}{2}\cos(\psi) \right]\right) \quad (3.8)$$

where N is the normalization factor chosen so that $\mathcal{K}(L, a = 0) = 1$ (note here we have taken $f(\psi) = 1$ as the boundary term does not influence the bulk physics). In the limit $L \to \infty$

$$\mathcal{K}(L, a) = \exp\left(\frac{\gamma_0(a)}{2}L\right) \quad \Rightarrow \quad \gamma_0(a) = 2\frac{\partial}{\partial L}\log \mathcal{K}(L, a) \quad (3.9)$$

It is convenient to discretize L so that $L = n\varepsilon$, where ε is the lattice spacing. Then the operation $\partial/\partial L$ can be performed directly on the LHS of Eq. (3.8) as

$$\gamma_0(a) = 2\frac{1}{n}\frac{\partial}{\partial\varepsilon}\log \mathcal{K}(L, a)$$

$$= \langle(\psi')^2\rangle + a\langle\cos(\psi)\rangle - \frac{1}{\varepsilon} \quad (3.10)$$

The last term arises because the normalization factor N depends on ε. This term cancels trivially with a simple ε divergence in the 1-loop graph for $\langle(\psi')^2\rangle$. We can now take the limit $\varepsilon \to 0$. The density, defined by Eq. (3.3), is given by

$$\rho = \frac{e^2 a}{2}\langle\cos(\psi)\rangle \quad (3.11)$$

and thus the second term in Eq. (3.10) corresponds to the free gas term. Hence, we have

$$P_{bulk} = \rho + \frac{e^2}{2}\left[\langle(\psi')^2\rangle - \frac{1}{\varepsilon}\right] \quad (3.12)$$

We define the Debye mass m by $m^2 = a/2$ and then

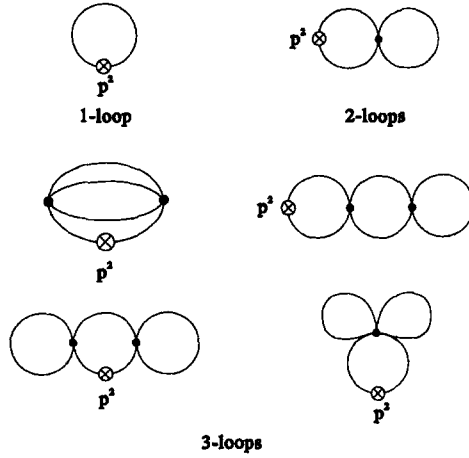$$\mathcal{K}(L, a) = \int d[\psi] \exp(-S[\psi]) \quad (3.13)$$

Fig. 1. The one-dimensional Feynman graphs up to three-loop order which contribute to the calculation of the bulk pressure in Eq. (3.12). The operator insertion $\otimes$ for $(\psi')^2$ is shown and corresponds to the insertion of the factor p^2 in the appropriate loop integral.

where overall irrelevant constant factors have been omitted, and

$$S[\psi] = \int_{-\infty}^{\infty} dx \left[\frac{1}{2} (\psi')^2 + \frac{1}{2} m^2 \psi^2 + \sum_{n=2}^{\infty} \frac{(-1)^{n+1} m^2}{(2n)!} \psi^{2n} \right] \tag{3.14}$$

A standard Feynman graph expansion of closed loops for $\langle (\psi')^2 \rangle$ can be obtained and hence the pressure can be calculated from Eq. (3.12). Standard dimensional analysis shows that the series obtained is in inverse powers of m and that a diagram with l loops behaves as m^{2-l}. To three-loop order we evaluate the diagrams shown in Fig. 1 and find

$$P_{bulk} = \rho + \frac{e^2}{2} \left(-\frac{m}{2} + \frac{1}{16} + \frac{3}{512m} \right) \cdots \tag{3.15}$$

In order to express P_{bulk} as a function of the density, ρ, we use Eq. (3.11) and calculate ρ in the loop expansion. As before, the diagrams with l loops behave as m^{2-l}. If P is calculated to l-loop order, then ρ is needed to $(l-1)$-loop order. To two-loop order we find

$$\rho = e^2 m^2 \left(1 - \frac{1}{4m} \right) \tag{3.16}$$

Note that, alternatively,

$$\rho = \frac{m}{2} \frac{\partial P_{bulk}}{\partial m} \tag{3.17}$$

and if we define $t = \log(m)$ and write $P_{bulk} = \rho + P_c$ then we have

$$\frac{d\rho}{dt} - 2\rho = -\frac{dP_c}{dt} \tag{3.18}$$

which has solution

$$\frac{\rho}{m^2} = \int_m^\infty \frac{1}{m'^2} \frac{dP_c}{dm'} dm' + e^2 \tag{3.19}$$

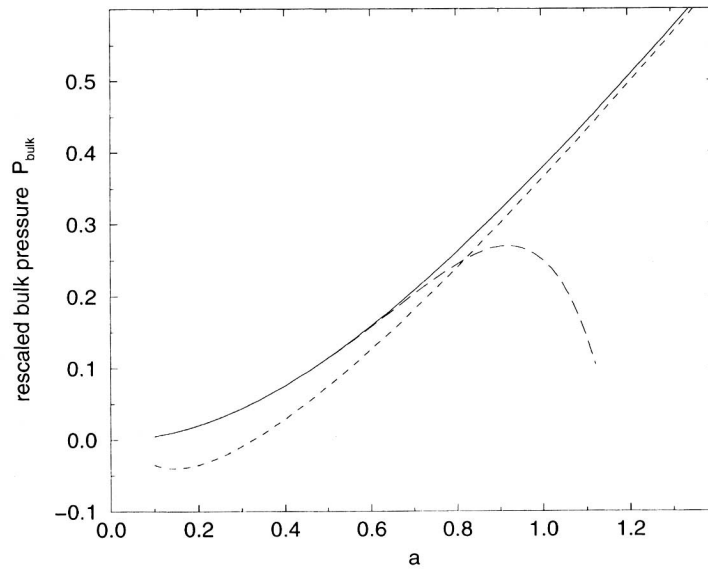where we have used the boundary condition that $\rho/m^2 \to e^2$ as $m \to \infty$.

Fig. 2. The bulk pressure P_{bulk}, scaled by $e^2/2$ versus $a = 4\mu/e^2$. The solid line is the exact computed curve and the dashed and long-dashed curves are the predictions of Eqs. (3.2) and (3.15), respectively. The predictions fit very well except in the region $0.7 < a < 1.1$.

Then $P(m)$ can be re-expressed as a series in $\sqrt{p/e^2}$:

$$P_{bulk} = p - \frac{1}{4} \sqrt{pe^2} + \frac{1}{1024} \sqrt{\frac{e^6}{p}} + \cdots \qquad (3.20)$$

This agrees with Lenard[2] and it is relatively easy to evaluate the loop expansion to higher orders to improve on Lenard's result. The second term is the familiar Debye–Hückel contribution and it should also be noted that the two-loop contribution is zero.

3.3. The Bulk Pressure

In Fig. 2 we show the numerically (see later) computed value for P_{bulk} compared with the predictions of the previous two sections. For convenience P_{bulk} has been scaled by a factor of $e^2/2$. As can be seen the curves from Eqs. (3.2) and (3.15) fit very well except in the region $0.7 < a < 1.1$ where even so the discrepancy is not very large.

4. THIN FILMS: FINITE-SIZE EFFECTS AND SURFACE CHARGE REGULATION

When the intersurface distance of the film becomes small in the sense that $\frac{1}{2}e^2L$ is no longer large, then we may not apply the thermodynamic result (3.1).

However if $\frac{1}{2}ae^2L$ and $\frac{1}{2}e^2L$ are both small, which is certainly the case for extremely small L, then one may expand the operator $\exp(LH)$ in powers of LH. To second order in LH one obtains

$$Z = 1 + 2\mu L\lambda + \frac{L^2}{2}(2\mu^2(\lambda^2 + 1) - \mu\lambda e^2) + O(L^3) \qquad (4.1)$$

thus yielding $\log(Z) \approx 2\mu L\lambda$ and $P_d = 2\mu\lambda - P_{bulk}$. Hence one has the limiting value of the disjoining pressure is negative if the value of λ is sufficiently small. However, one has the bound that $\gamma_0(a) < a$ and hence $P_{bulk} < 2\mu$ thus

$$\lim_{L \to 0} P_d > 2\mu\lambda - 2\mu \qquad (4.2)$$

Hence the film certainly has a positive disjoining pressure at small differences if $\lambda > 1$. The stability of the film at small separations is determined by

$$\lim_{L \to 0} \frac{\partial P_d}{\partial L} = 2\mu^2(1 - \lambda^2) - \mu\lambda e^2 \qquad (4.3)$$

If this term is positive then the film collapses to the point thickness $L = 0$. For this to happen one must have

$$\lambda < 1 \tag{4.4}$$

and

$$\mu > \frac{\lambda e^2}{2(1 - \lambda^2)} \tag{4.5}$$

The value of the surface charge σ is given by

$$\sigma = -e \frac{1}{2} \frac{\partial}{\partial \lambda} \log(Z) = -\lambda e \langle \exp(-i\phi(0)) \rangle = -eL\lambda\mu \tag{4.6}$$

Hence over short distances the surface charge decays linearly as the two surfaces are brought together.

5. INTERMEDIATE REGIME

In the regime between very thick and very thin films we shall resort to a numerical analysis of the problem. There are two methods of interest which we detail in the following sections. The figures in this section are shown in units where L is scaled by $e^2/2$. That is, a factor of $e^2/2$ is absorbed into all length variables.

5.1. The Mathieu Function Method

The disjoining pressure and other properties of the film can be calculated using the even and odd Mathieu functions that are the eigen-functions of H^* defined in Eq. (2.28). The kernel $\mathcal{K}(L, a)$ defined in Eq. (3.8) can be computed as an expansion on the Mathieu function by resolution of the identity on the basis of these states. In this way the disjoining pressure may in general be written as

$$P_d(L) = -\frac{e^2}{2} \frac{\sum_{n=1}^{\infty} (\gamma_0(a) - \gamma_n(a)) c_n^2 \exp((e^2/2) \gamma_n(a) L)}{\sum_{n=\infty}^{\infty} c_n^2 \exp((e^2/2) \gamma_n(a) L)} \tag{5.1}$$

where

$$c_n = \int_0^{2\pi} d\phi \, \chi_n(\phi) \exp(\lambda \exp(-i\phi)) \tag{5.2}$$

If the eigenvalues of H are arranged in descending order i.e., $\gamma_0 > \gamma_1 > \gamma_2 \cdots$, the corresponding eigenfunctions are even about π for n even and odd about π for n odd. Hence c_n is purely real for n even and purely imaginary for n odd. If $\lambda = 0$ then $c_n = 0$ for n odd and hence P_d is always negative, hence the force between the two interfaces is always attractive. One sees from the above expression that it is the even wave functions which are attractive and the odd wave functions which are repulsive (as the denominator on the RHS of (5.1) is Z and hence positive). At long distances

$$P_d \sim -\frac{e^2}{2} \frac{c_1^2}{c_0^2} (\gamma_0 - \gamma_1) \exp\left(\frac{e^2}{2} L(\gamma_1 - \gamma_0)\right) > 0 \qquad (5.3)$$

Hence for a non-zero λ the long distance disjoining pressure is always positive since $c_1^2 < 0$. It is clear however that the disjoining pressure may become negative at smaller values of L.

The anion and cation number densities as a function of x, the distance through the film, may also be calculated by taking functional derivatives with respect to the fugacities. Denoting these densities respectively by ρ_+ and ρ_- we find

$$\rho_\pm = \frac{1}{2\pi Z} \sum_{n,m} \mu \langle f^* \mid \chi_n \rangle \exp\left(\frac{e^2}{2} \gamma_n x\right) \langle \chi_n \mid e^{\pm i\phi} \mid \chi_m \rangle$$

$$\times \exp\left(\frac{e^2}{2} \gamma_m(L - x)\right) \langle \chi_m \mid f \rangle \qquad (5.4)$$

where

$$\langle \psi \mid \chi \rangle = \int d\phi \, \psi^*(\phi) \chi(\phi) \qquad (5.5)$$

We are able to construct both the even and the odd Mathieu functions and their eigenvalues for any value of a using Given's method for diagonalizing a tri-diagonal matrix. The eigenfunctions of H^* are found on a discretization of the interval $[0, 2\pi]$ and the appropriate matrix elements in Eqs. (5.1), (5.4) can be calculated numerically.

5.2. Fourier Method

It turns out that there is a more direct method to calculate the disjoining pressure which exploits the periodicity inherent in the system. This

method is especially effective for low temperature (small e). It does, however, become much more complicated when other observables such as the density profiles are being calculated. Expanding K in terms of its Fourier modes, i.e. writing

$$K(\phi \mid x) = \exp(ax) \sum_{n = -\infty}^{\infty} b_n(x) \exp(in\phi) \tag{5.6}$$

one has that

$$b_n(0) = \frac{\lambda^{-n}}{(-n)!} \quad \text{for} \quad n \leqslant 0$$

$$= 0 \quad \text{for} \quad n > 0 \tag{5.7}$$

and the b_n evolve via the equation

$$\frac{db_n}{dx} = -n^2 b_n + a(b_{n+1} + b_{n-1} - 2b_n)/2 \tag{5.8}$$

Finally the partition function is given by

$$Z = \exp(aL) \sum_{n=0}^{\infty} \frac{\lambda^n}{(n)!} b_n(L) \tag{5.9}$$

In this regime we shall also be interested in the mean value of the surface charge σ.

$$\sigma = -\lambda e \langle \exp(-i\phi(0)) \rangle$$

$$= -\frac{\lambda e}{Z} \frac{1}{2\pi} \int_0^{2\pi} d\phi_0 \exp(-i\phi_0) \, f(\phi_0) \exp(LH) \, f(\phi_0) \tag{5.10}$$

In terms of the Fourier expansion this becomes

$$\sigma = -\frac{\lambda e}{Z} \exp(aL) \sum_{n=0}^{\infty} \frac{\lambda^n}{(n)!} b_{n+1}(L) \tag{5.11}$$

The disjoining pressure may be computed similarly.

In what follows we shall consider three cases which are paradigms for the different regimes of high, intermediate and low temperature. Since we have set $kT = 1$, high T corresponds to a small charge parameter, e and

vice-versa. Apart from an overall dimension-carrying factor the results depend on e and μ through the combination $a = 4\mu kT/e^2$, and in what follows we choose $\mu = 1$ and hence in our units $a = 4/e^2$. The three regimes of temperature are characterized by the three values of charge: $e = 0.1, 1, 4$.

5.3. $e = 0.1$, $a = 400$

From Eq. (3.15) the bulk pressure is $P = 1.926$. The major correction to the free particle pressure, $P_{free} = 2$, is the Debye-Hückel term and the two and three-loop contributions are a correction of only $\Delta P = 0.003$. In Figs. 3 and 4 we show the pressure P versus film thickness L for various values of λ in the range 0.9 to 1.2. Also plotted is the prediction for the bulk pressure to which all curves should be asymptotic. As can be seen there is a collapse in all cases shown for λ. The details of the collapse differ, however, as λ increases. For the lower values of λ the collapse is to a film of zero thickness which would, of course, be dominated by the detailed structure of the surface physics which we have subsumed in to a layer of zero thickness. Two maxima are clearly visible for $\lambda = 0.93, 0.95$. The one at larger L is the location of the ordinary collapse point. The maximum at
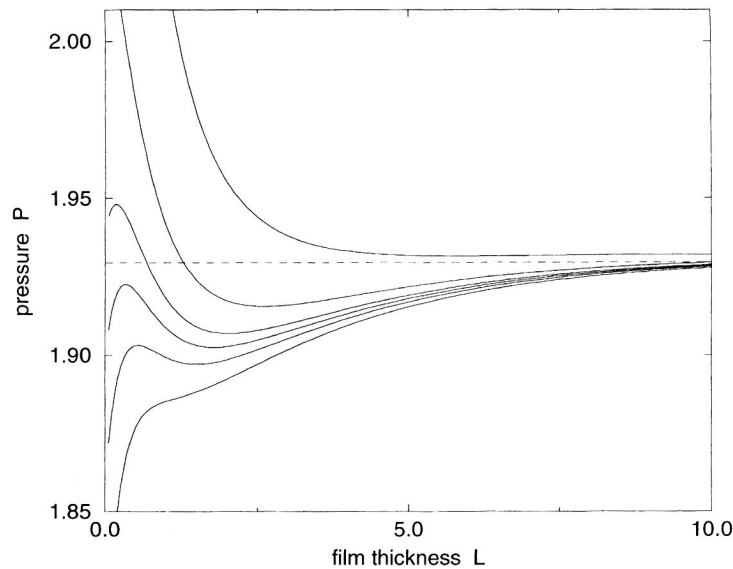

Fig. 3. The pressure P versus film thickness L for $kT = 1.0$, $e = 0.1$ and $\mu = 1.0$. for $0 < L \leqslant 10.0$. The different curves are for $\lambda = 0.9$, 0.93, 0.95, 0.97, 1.02, 1.2 which respectively correspond to the curves from lowest to highest pressure at any given L. The phenomenon of primary and, in some cases, secondary collapse are clearly visible.
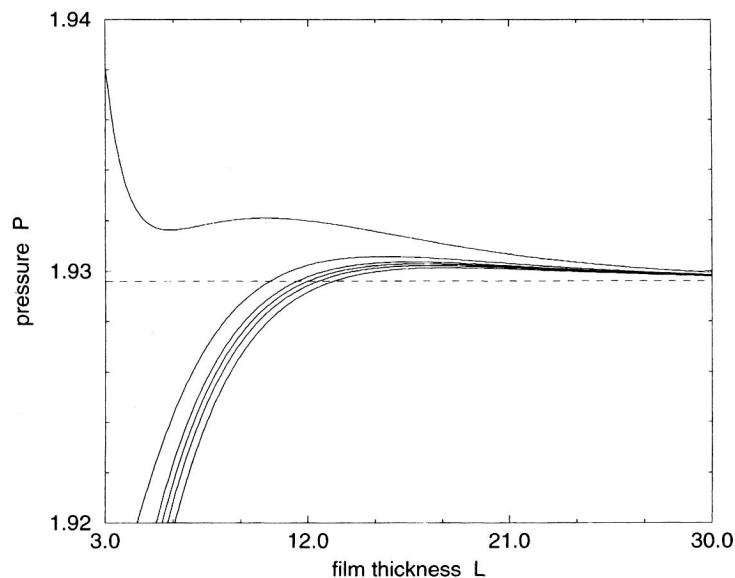
Fig. 4. The curves shown in Fig. 3 extending to larger L to highlight the region of primary collapse. As in Fig. 3 the higher the value of λ the higher the pressure at given L.

smaller L and the consequent multiple-valuedness of the curve in L versus P in this region implies a hysteresis phenomenon as P is cycled for very thin films. This kind of effect is reminiscent of a first-order transition which predicts that for a 3D film there will be domains of different thicknesses which will grow or contract like 2D bubbles. Of course, it remains to be seen whether intuition from 1D survives for the realistic 3D case.

For the curves with larger values of λ plotted, the collapse is to a thinner film but not to one of zero thickness. As λ increases the maximum at small L eventually disappears and for much larger λ the collapse phenomenon itself disappears.

In Fig. 5 we shown the surface charge σ defined in Eq. (5.10) as a function of L. There is no feature which hints at the presence of the collapse phenomenon appearing in the associated pressure curves, but in all cases σ decreases with L (charge regulation). For small L the behavior agrees well with the prediction of Eq. (4.6).

The anion and cation densities have been computed as a function of x for various values of L using Eq. (5.4). For $e = 0.1$ the variation with x is mild and shows no features of note. We show the midplane values for each species as a function of L and for various values of λ in Fig. 6.
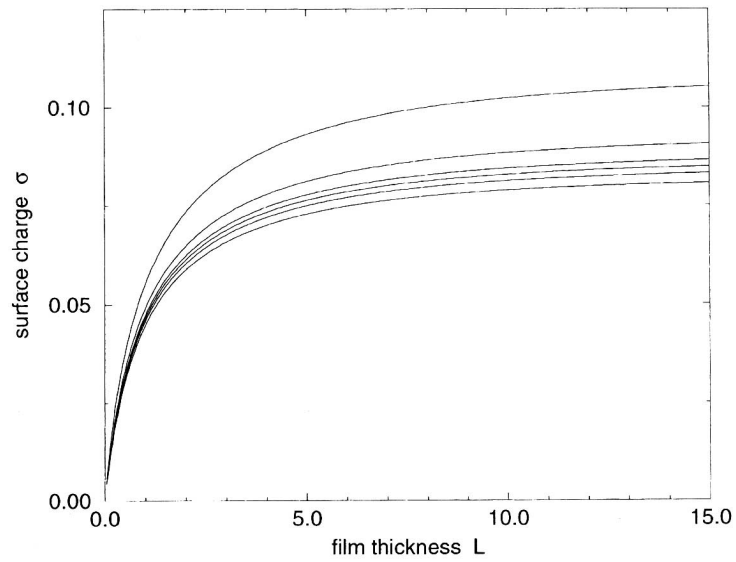
Fig. 5. The surface charge σ defined by Eq. (4.6) versus film thickness L for $kT = 1.0$, $e = 0.1$ and $\mu = 1.0$. The different curves are for $\lambda = 0.9, 0.93, 0.95, 0.97, 1.02, 1.2$ corresponding to the curves from lowest to highest σ. There is no feature which hints at the presence of the collapse phenomenon appearing in the pressure curves shown in Figs. 3 and 4.
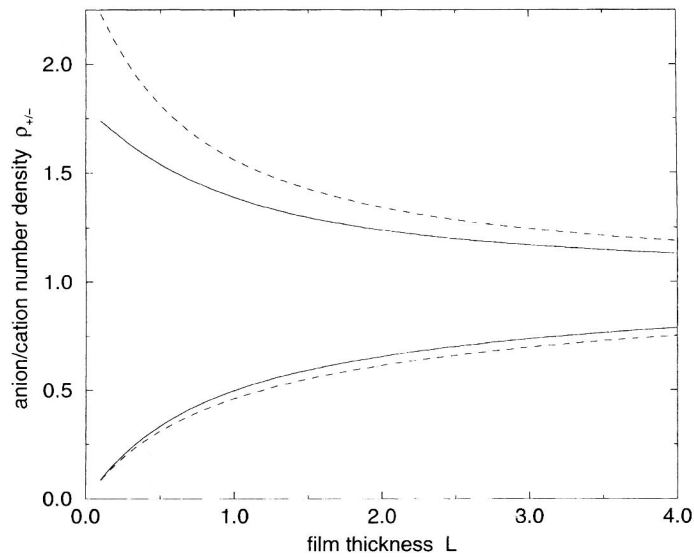

Fig. 6. The midplane anion (upper curves) and cation (lower curves) densities as a function of film thickness L, for $e = 0.1$, $\mu = 1$, $\lambda = 0.9$ (solid) and 1.2 (dashed).

It is interesting to note that both methods described in Sections 5.1 and 5.2 were used to calculate the disjoining pressure. However, while 10 Fourier modes were amply sufficient, the number of Mathieu modes needed was 40. In particular this large number of modes was found necessary to reproduce the secondary collapse maxima shown in Fig. 3.

5.4. $e = 1.0$, $a = 4$

As in the previous section the pressure P versus L is plotted in Fig. 7 for values of λ in $0.3 \leqslant \lambda \leqslant 0.8$ which span a region of collapse. In this case there is just one point of collapse to a film of zero thickness (in our approximation) and which disappears for λ between 0.7 and 0.8. From Eq. (3.15) the bulk pressure is predicted to be $P_{bulk} = 1.3262$. From the exact calculation we find $P_{bulk} = 1.32584$ which is in good agreement with the prediction. To guide the eye the computed asymptotic value is shown in Fig. 7. These pressure curves are well reproduced by the Mathieu function method with as few as 8 modes. Unlike the case in the previous section $a = 4$ is sufficiently small that the physics is dominated by the lowest-lying
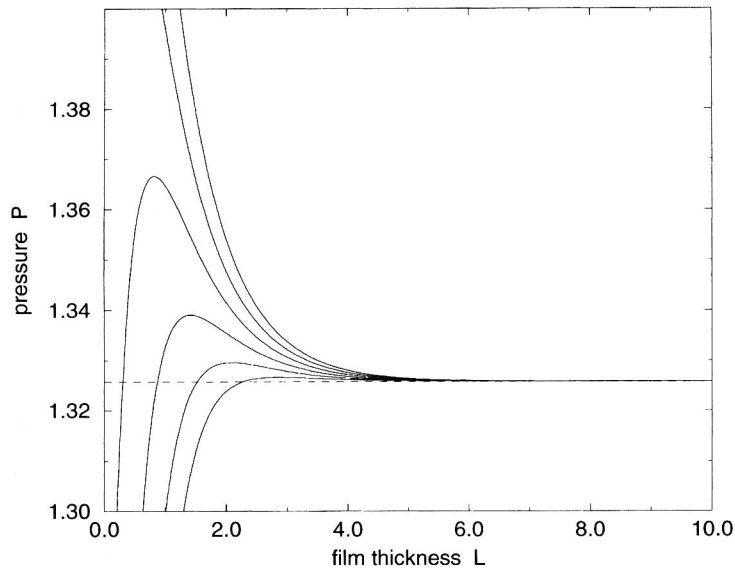

Fig. 7. The pressure P versus film thickness L for $kT = 1.0$, $e = 1.0$ and $\mu = 1.0$. The different curves are for $\lambda = 0.3, 0.4, 0.5, 0.6, 0.7, 0.8$ which respectively correspond to the curves from lowest to highest pressure at any given L. The collapse phenomenon occurs for the smaller λ values and disappears between $\lambda = 0.7$ and $\lambda = 0.8$.
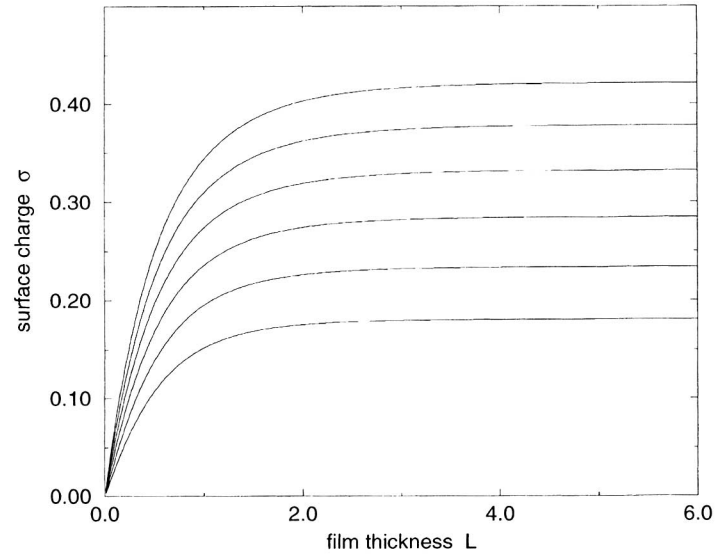
Fig. 8.   The surface charge σ defined by Eq. (4.6) versus film thickness L for $kT = 1.0$, $e = 0.1$ and $\mu = 1.0$. The different curves are for $\lambda = 0.9, 0.93, 0.95, 0.97, 1.02, 1.2$ corresponding to the curves from lowest to highest σ. There is no feature which hints at the presence of the collapse phenomenon appearing in the pressure curves shown in Figs. 3 and 4.
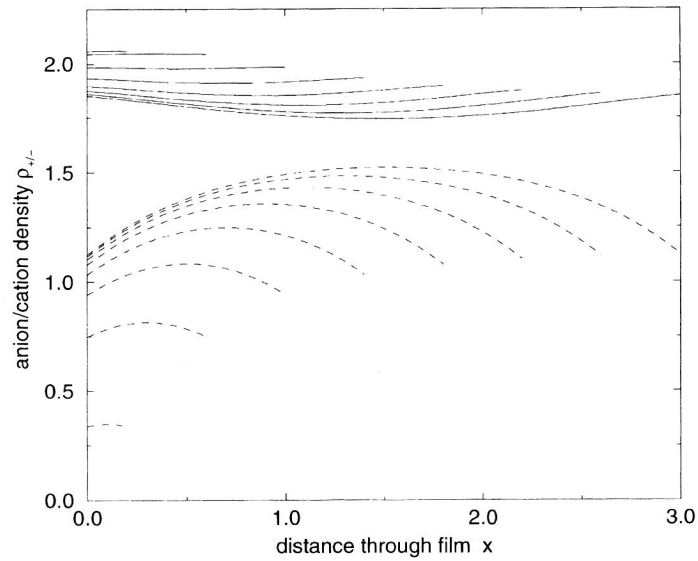

Fig. 9.   The anion (solid curves) and cation (dashed curves) densities as a function of distance x through the film for $e = 1.0$, $\mu = 1$, $\lambda = 0.95$ and for various film thickness L.

Mathieu eigenfunctions. This is mainly due to the fact that λ is smaller and so the overlap $\langle \chi_n \mid f \rangle$ falls off more sharply with n. This in turn means that the pressure peak occurs for larger L than in the $a = 400$ case. However, the large-a result for the bulk pressure, Eqs. (3.15), (3.20) still holds very well in this region which means that the Debye–Hückel approximation is good.

The surface charge σ is plotted in Fig. 8 and, as in the previous case, there are no features associated with the pressure maxima of Fig. 7.

The anion and cation number densities as a function of distance, x, through the film are shown in Fig. 9 for $\lambda = 0.5$. These quantities were calculated using Eq. (5.4). The anion (cation) curves are the higher (lower) set in this figure. There are no unusual features and the curves for the other values of λ in $0.3 \rightarrow 0.8$ are of similar form.

5.5. $e = 4.0$, $a = 0.25$

The pressure P is plotted versus L for $\lambda = 0.12$, 0.121, 0.122, 0.123 in Fig. 10. The collapse region is again evident but it should be noted that it occurs only for a very narrow range of λ values. Of course, λ is a parameter
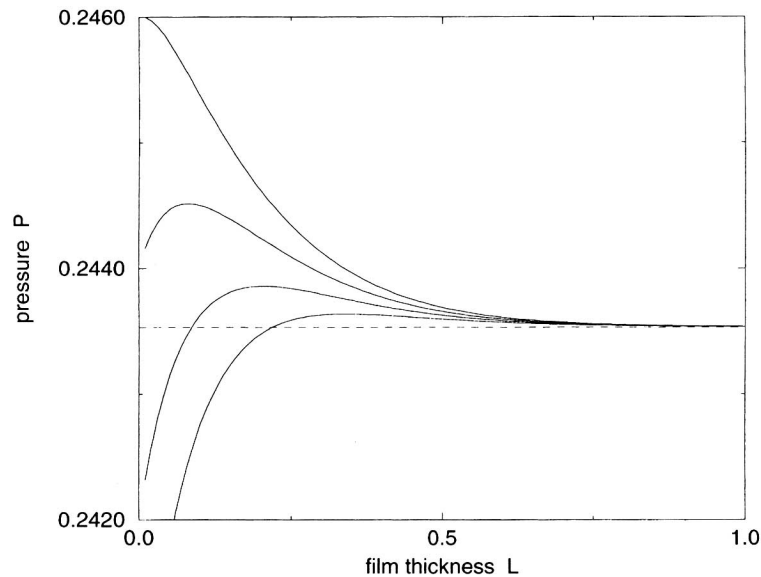

Fig. 10. The pressure P versus film thickness L for $kT = 1.0$, $e = 4.0$ and $\mu = 1.0$. The different curves are for $\lambda = 0.12, 0.121, 0.122, 0.123$ which respectively correspond to the curves from lowest to highest pressure at any given L. The collapse phenomenon occurs for the smaller λ values and disappears between $\lambda = 0.122$ and $\lambda = 0.123$.

that is determined by other variables and is not fixed externally. The bulk pressure is no longer given by the large-a expression (Eqs. (3.15) and (3.20)) but is well fitted by the small-a result (Eqs. (3.2) and (3.5)). The prediction is $P_{bulk} = 0.243529$ and the computed value is $P_{bulk} = 0.243531$. This value is shown for reference in Fig. 10.

The curves for the surface charge, σ, are similar to those of previous sections and are not reproduced here. The small L behavior is again consistent with Eq. (4.6).

The anion and cation number densities (Eq. (5.4)) are plotted for $\lambda = 0.123$ and $L = 0.1$, $0.51.1$ in Fig. 11. It is interesting to note that for both species the density falls sharply at the film surface and the anion density reaches a peak for the thicker films which is located only a short distance into the film. The position and shape of this peak is independent of thickness L and seems to be a universal feature of the low temperature case. Only the lowest 4 Mathieu modes make an appreciable contribution since the effective charge is large and from Eq. (5.4) this causes a strong exponential suppression on all but the lowest modes (note that in Eq. (5.4) a factor of $e^2/2$ is absorbed into all lengths). Also, the values of λ in the collapse region decrease as e increases and so the surface function $f(\phi)$ (Eq. (2.22)) oscillates less fast and only has appreciable overlap with the lowest modes. For these reasons the species number densities are dominated
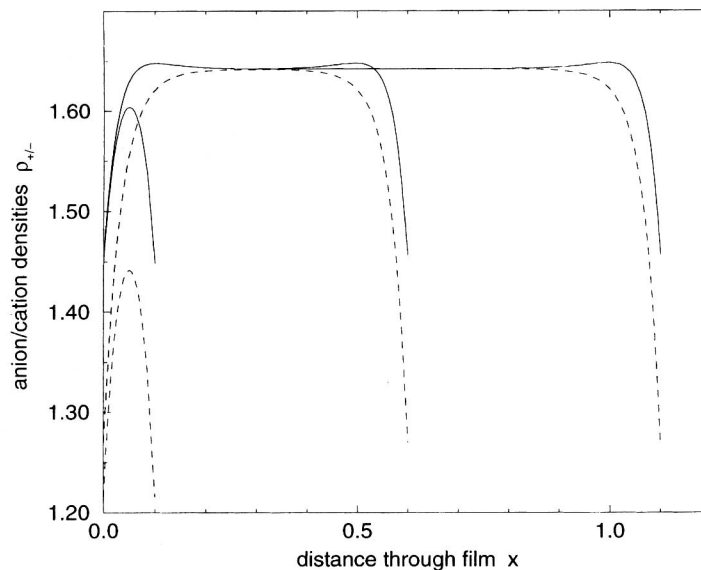

Fig. 11. The anion (solid curves) and cation (dashed curves) densities as a function of distance x through the film for $e = 4.0$, $\mu = 1$, $\lambda = 0.123$ and for film thicknesses $L = 0.1, 0.51.1$.

by the contributions from the lowest modes and so show more structure at low temperature than at high temperature. This is to be expected since the electrostatic energy dominates the thermal energy. We have observed similar maxima in the density profiles for other values of e if λ is sufficiently small. This is due again to the dominance of only a very few low-lying Mathieu modes.

6. COMPARISON WITH POISSON–BOLTZMANN THEORY

The Poisson–Boltzmann (PB) theory for our system may either be derived directly by standard thermodynamic techniques,[8, 9] or as the mean field theory for the field theory (2.9). The theory has been used in a wide context in soft condensed matter physics and in particular to analyze the behavior of soap films in refs. 11–13, and also in the context of colloidal stability.[8, 9] In general it is fair to say that it has been reasonably successful in predicting the physics of systems where interplane distances are reasonably large and for monovalent ionic species.[15]

The resulting equations are (again scaling so that $\beta = 1$)

$$\frac{d^2\phi}{dx^2} = 2\mu e \sinh(e\phi) + \lambda e[(\delta(x)\exp(e\phi(0))) + \delta(x - L))\exp(e\phi(L))] \qquad (6.1)$$

where here ϕ is the mean field electrostatic potential. Assuming symmetry about the point $L/2$ (however see the comments in the conclusion) and using the condition of electroneutrality, the boundary conditions are

$$\frac{d\phi}{dx}\bigg|_{0, L} = \frac{d\phi}{dx}\bigg|_{L/2} = 0 \qquad (6.2)$$

Interestingly ϕ appears as a purely imaginary saddle point of the theory (2.9). In the region $[0^+, L^-]$ the above equation reduces to

$$\frac{d^2\phi}{dx^2} = 2\mu e \sinh(e\phi) \qquad (6.3)$$

with the boundary conditions

$$\frac{d\phi}{dx}\bigg|_{L/2} = 0 \qquad (6.4)$$

and

$$\left.\frac{d\phi}{dx}\right|_0 = \lambda e \exp(e\phi(0)) = -\sigma \tag{6.5}$$

where σ is the surface charge. It easy to show that the mean field free energy over the bulk is[8]

$$F_{MF} = \int_0^L (\phi')^2 \, dx - (2\lambda \exp(e\phi(0)) + 2\mu L(\cosh(e\phi(L/2)) - 1)) \tag{6.6}$$

In addition, we find

$$P_d = 2\mu(\cosh(e\phi_m) - 1) \tag{6.7}$$

where $\phi_m = \phi(L/2)$ is the midplane potential. One immediately sees that in the case $\lambda = 0$ then $\phi = 0$ is a solution and the film is always marginally stable in the sense that $P_d = 0$. In general any non-zero λ gives a non-zero value of ϕ_m and hence the film is always stable for non-zero λ. This is clearly at variance with the exact results derived here. Moreover, the mean field bulk pressure is $P_{bulk} = 2\mu$ which is only applicable to the limit $e \to 0$ or, equivalently, $a \to \infty$.

In general one must resort to a numerical solution of the above mean field equations. However in the case where L is small such that ϕ varies only slightly we may use the approximation,

$$\phi = \phi_m + C\left(x - \frac{L}{2}\right)^2 \tag{6.8}$$

Substituting this into Eq. (6.3) yields $C = \mu e \sinh(\phi_m)$. Using this in the boundary condition (6.5) then yields

$$\mu L \sinh(e\phi_m) = -\lambda \exp(e\phi_m) + O(L^2) \tag{6.9}$$

Solving this yields

$$\phi_m = -\frac{1}{2e} \log\left(\frac{2\lambda}{\mu L} + 1\right) \tag{6.10}$$

Hence in this limit

$$P_d(L) \sim \sqrt{\frac{2\lambda\mu}{L}} \tag{6.11}$$

and

$$\sigma \sim -e \sqrt{\frac{L\mu\lambda}{2}} \qquad (6.12)$$

One sees that while the surface charge σ does decay to zero it does so as $L^{1/2}$ in comparison with the exact result (4.6). In addition the disjoining pressure (6.11) actually diverges rather than tending to a constant.

For infinitely thick films one may use the condition that $\phi_m \rightarrow 0$ in order to calculate the surface potential (we simply use the first integral of Eq. (6.3)). In this case the surface potential is given by the equation

$$\cosh(e\phi(0)) - \frac{1}{4\mu} \lambda^2 e^2 \exp(e\phi(0)) = 1 \qquad (6.13)$$

from this we find that the physical solution is

$$\phi(0) = -\frac{1}{e} \log(1 + \lambda e/\sqrt{2\mu}) \qquad (6.14)$$

giving a surface charge

$$\sigma = \frac{-\lambda e}{1 + \lambda e/\sqrt{2\mu}} \qquad (6.15)$$

At intermediate distances one has to numerically solve the PB equations. For the cases discussed in Section 5 there is no agreement at all between the numerical solution to the PB equation and the exact result. This is to be expected since there is no collapse predicted by the PB equation. However, there is no agreement even on the rising part of the pressure curve at L much greater than that at the pressure maximum. Also, the values of P_{bulk} are not close to the mean-field prediction of $P_{bulk}^{MF} = 2.0$ although for $e = 0.1$ this value is approached. Nevertheless, in this latter case there is still a large disagreement between the exact and mean-field curves. Indeed, we have investigated very small values of e for a large range of λ values but have not found any reliable agreement between the exact theory and the PB equation. The PB equation may be applicable for even smaller values of e than we have investigated, indeed a naive analysis of the applicability of the saddle point method for the theory (2.9) seems to suggest that one requires a to be finite but with either $\mu \gg 1$ or $e^2 \ll 1$, thus giving either μ or $1/e^2$ as the large parameter justifying the saddle point method. In the cases we have analyzed, mean-field theory and the PB

equation are of very little value in the analysis of the one-dimensional Coulomb gas.

7. CONCLUSIONS

In conclusion we have derived an exact solution for the one-dimensional Coulomb gas with boundary effects. Surprisingly the mere presence of a boundary but without any adhesion term leads to a negative disjoining pressure and the resulting film will tend to collapse. When $\lambda > 0$ we have shown that at sufficiently large distances the disjoining pressure must be positive, and hence a stable *common* film regime exists. However, if the value of λ is not too large a collapse phenomena may occur where the disjoining pressure decreases as the surfaces come together. The disjoining pressure may even become negative signaling the onset of strong attractive forces in the system; this may well be the one-dimensional version of the collapse to a NBF seen in experimental systems. We have also seen the *possibility of secondary collapses in the parameter ranges we have studied*; it would be interesting if one could find an experimental system exhibiting a secondary collapse. In principle multiple collapses are possible, but we are yet to see more than two.

Poisson–Boltzmann theory predicts a stable film for any non-zero value of λ and in addition the calculated mean field disjoining pressure is larger that that of the exact calculation. Taking into account the full theory and all its correlations does indeed introduce an attractive interaction over and above the mean field result, in accordance with the calculations made in three dimensional systems using techniques beyond mean field theory.[5, 6, 14] We would like to comment here that in our solution of the mean field equations we have, as is done throughout the literature, always assumed that the mean field solution is symmetric about the midplane of the film. In physical terms this seems quite plausible for thick films where the two planes do not interact and hence there can be no breaking of spatial symmetry. The variant of mean field theory used in refs. 12 and 13 uses this symmetric solution and the theory describes extremely well both surface tension data for SDS bulk solutions and the disjoining pressure isotherms up to the point where the collapse occurs. One may show[16] that in the field theoretic sense that the mean field solutions we have found here and in refs. 12 and 13 are indeed stable local minima of the free energy and hence they at least describe a metastable state. The fact that the mean field solutions work so well in this context up to the collapse point suggest that another mean field solution with a broken spatial symmetry and possibly with a complex part may appear with a lower free energy than that of the symmetric real solution. This would also be consistent with the experimental

indications (and indeed conclusions that may be drawn from our exact solutions in 1D) that the transition to a Newton Black Film is of first order. Work on this problem is currently under progress.[16] Also of interest would be to test the validity of the linearized Poisson–Boltzmann equations which have the virtue of obeying certain sum rules which are violated by the full nonlinear equations.[20]

ACKNOWLEDGMENTS

REFERENCES

1. S. Edwards and A. Lenard, *J. Math. Phys.* **3**:778 (1962).
2. A. Lenard, *J. Math. Phys.* **2**:682 (1961).
3. S. Prager, *Advances in Chemical Physics IV*, 201, Wiley (Interscience), New York, (1962).
4. E. H. Lieb and D. C. Mattis, *Mathematical Physics in One Dimension*, Perspectives in Physics, (Academic Press), New York and London, (1966).
5. R. Kjellander and S. Marcelja, *J. Phys. Chem.* **90**:7, 1230 (1986).
6. O. Spalla and L. Belloni, *Phys. Rev. Lett.* **74**:13 (1995).
7. F. Cornu and B. Jancovici, *J. Chem. Phys.* **90**:4, 2444 (1989).
8. J. Israelachvili, *Intermolecular and Surface Forces* (Academic Press, 1992).
9. I. B. Ivanov (ed.), *Thin Liquid Films (Fundamentals and Applications)*, Surfactant Science Series (Marcel Dekker, Inc.), 1988; J. Lykelma, *Fundamentals of Interface and Colloid Science (Volume 1: Fundamentals)* (Academic Press, 1991).
10. J. T. Davies, *Proc. Roy. Soc. A* **245**:417 (1958).
11. D. Exerowa, T. Kolarov, and Khr. Khristov, *Colloids and Surfaces* **22**:171 (1987).
12. D. S. Dean and D. Sentenac, *Europhys. Lett.* **38**:9, 645 (1997).
13. D. S. Dean and D. Sentenac, *J. Colloid Interface Sci.*, submitted
14. R. Podgornik, *J. Chem. Phys.* **91**:9 (1989).
15. D. Andelman, *J. Phys. Chem.* **100**:32, 13732 (1996).
16. D. S. Dean, R. R. Horgan, and D. Sentenac, work in progress.
17. Abramowitz and Stegun, *Handbook of Mathematical Functions* (Dover Publications, 1964).
18. R. D. Coalson and A. Duncan, *J. Chem. Phys.* **97**:5653 (1992).
19. N. Ben-Tai and R. D. Coalson, *J. Chem. Phys.* **101**:5148 (1994).
20. We thank B. Jancovici for drawing our attention to this.